SCIENCE CHINA
Information Sciences

• RESEARCH PAPER •

September 2022, Vol. 65 192205:1–192205:13
https://doi.org/10.1007/s11432-021-3338-0

Model predictive control with input disturbance and guaranteed Lyapunov stability for controller approximation

Yanye WANG[1,2], Shaoyuan LI[1,2] & Yi ZHENG[1,2*]

[1]*Department of Automation, Shanghai Jiao Tong University, Shanghai* 200240*, China;*
[2]*Key Laboratory of System Control and Information Processing, Ministry of Education of China, Shanghai* 200240*, China*

Received 11 February 2021/Revised 21 May 2021/Accepted 4 August 2021/Published online 29 August 2022

Abstract An approximation method that can lower the computational complexity is presented to reduce the processing time of model predictive control (MPC). The effects of the inaccurate inputs, which are caused by the approximation errors, are reflected as input disturbances and are considered in the design of the controller. The closed-loop system's stability is guaranteed by a restricted Lyapunov-based constraint and input constraints, ensuring that the states will be eventually bounded at a certain confidence level. According to this paper, the effects of the bounded disturbance can be observed via a change in the stability region. The relationship between the regions of the normal and approximated systems is highlighted. The proposed MPC with input disturbance and guaranteed Lyapunov stability is employed in a chemical process, and the simulation results indicate the efficiency of the proposed method.

Keywords model predictive control, Lyapunov-based MPC, control approximation, learning-based control, nonlinear system

Citation Wang Y Y, Li S Y, Zheng Y. Model predictive control with input disturbance and guaranteed Lyapunov stability for controller approximation. Sci China Inf Sci, 2022, 65(9): 192205, https://doi.org/10.1007/s11432-021-3338-0

1 Introduction

Control optimization in nonlinear systems has attracted wide publicity, and many optimization methods have been applied in several industrial processes successfully [1–4]. As one of the optimization control methods, model predictive control (MPC) can solve an optimization problem with large multivariate constraints within a finite prediction horizon in each sampling time. It can explicitly accommodate constraints [5, 6]. Therefore, it is widely recognized as a practical, high-performance control technology. It has been successfully employed in several linear and nonlinear systems in the process industries and is gaining popularity [7–9]. However, one major drawback limiting its online application is that the optimization problem with large multivariate constraints can be time-consuming [10]. Hence, several projects are undertaken to increase computational speed. Machine learning has recently emerged as a popular method to emulate a well-designed controller and optimize the original controller design [11–13].

Several studies have utilized machine learning methods to approximate the MPC control law (i.e., the control action obtained by solving the optimization problem of MPC). Cseko et al. [14] presented a radial basis function-based neural network approximation to replace the explicit MPC controller. Lucia and Karg [15] have used deep learning techniques to develop a robust nonlinear MPC controller. Cao and Gopaluni [16] proposed a new "optimize and train" method for the large-scale problems based on the deep neural network approximation of the MPC control law. These studies aim at developing effective computational methods through the learning-based MPC for real-time application and solving large-scale problems. The influence of the approximation may not be based on the main object. Chen et al. [17] guaranteed the approximated control inputs by projecting them onto the polyhedral region related to

* Corresponding author (email: yizheng@sjtu.edu.cn)

the maximum positive invariant set of the system while they indicate the need to consider stability. Finally, Hertneck et al. [10] presented a robust MPC design considering the statistical learning bounds. Furthermore, the stability analysis is performed to guarantee robust inputs.

The effect of approximation in the Lyapunov-based MPC (LMPC) is also considered in this paper. Because structural errors are always present, the learning-based controller can be considered an approximation (not exact match) of the original one. The errors are determined by the chosen model type, and the obtained dataset is used in the learning process. The approximation error can be thought of as the input disturbance of the system, which will affect the performance of the closed-loop system. With input disturbance, the system's recursive feasibility and stability should be re-evaluated to meet the system's constraints.

In the feasibility and stability analysis of MPC problems, the disturbance of the controlled system may affect the control performance, such as the external disturbance and time delays [18–21]. Some studies are conducted to tackle these problems and ensure stability. Pannocchia et al. [22] presented that systems with soft terminal region constraints controlled by suboptimal MPC can be inherently robust. Allan et al. [23] provided sufficient conditions on a well-chosen initial guess for robust stability in suboptimal MPC with hard terminal region constraints. Pourdehi and Karimaghaee [24] proposed a systematic Lyapunov-based approach for reset control of the nonlinear time-delay, for which the stability is ensured by Lyapunov-stability theory. Choomkasien et al. [25] designed MPC for an industrial process with input time delay. Thus, analyzing the stability with the existence of various disturbances is crucial. Developing an MPC method with guaranteed feasibility and stability is meaningful for the systems with input disturbance caused by the approximation.

An approximation method is presented in this paper to increase the computational speed of the controller with guaranteed feasibility, where the approximation errors are bounded in certain confidence. The input disturbance of the system reflects the deviation of the controller approximation. The influence of input disturbance on a Lyapunov-based controller is discussed. Considering the stability of the closed-loop system, the regions where the state can be ultimately bounded are redefined. Compared with those articles whose main purpose is achieving reductions in computational time of MPC, our work further considers the stability problems caused by the approximation. In [10], the design of robust MPC is presented considering stability analysis. However, we propose the design of the Lyapunov-based MPC under the influence of approximation error, and the result can be different owing to the inconsistency in the principle of ensuring system stability.

The major advantages of the proposed LMPC scheme are listed as follows.

- The proposed MPC considers the input disturbances derived from the approximation errors and guarantees the stability of the closed-loop system at certain confidence. The stability conditions of the proposed MPC-controlled system are also analyzed. It differs from those without the inputs disturbance because the stability regions are redefined.
- An implementation method realized through a machine learning algorithm is proposed, where the approximate errors are limited inside an acceptable range with a certain confidence level according to Hoeffding's inequality.
- The designed controller can be used for both tracking and economic optimization.

This paper is organized as follows. In Section 2, we review key concepts and notations before analyzing nonlinear systems with input disturbance. In Section 3, the MPC controller is designed, and the stability analysis is performed. Section 4 describes an implementation method that uses Hoeffding's inequality to simulate an approximate controller. The controller is employed in a continuous stirred tank reactor (CSTR), and the simulation results are presented in Section 5. Finally, a conclusion is given in Section 6.

2 System and preliminaries

2.1 Notation

$|\cdot|$ denotes Euclidean norm of a vector; a continuous function $\alpha : [0, \alpha) \to [0, \infty)$ is said to belong to class κ if it is strictly increasing and $\alpha(0) = 0$; we use Ω_ρ to denote the set $\Omega_\rho := \{x \in \mathbb{R}^{n_x} | V(x) \leqslant \rho\}$; the operator '/' denotes $A/B = \{x \in \mathbb{R}^{n_x} : x \in A, x \notin B\}$.

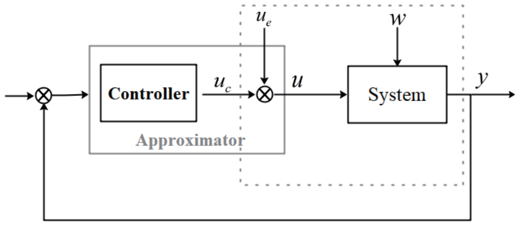

Figure 1 The nonlinear systems with input disturbance.

2.2 Class of nonlinear systems

The structure of the nonlinear systems is shown in Figure 1, the controller is approximated by learning techniques, and the output of the approximate controller serves as the input of the system. Therefore, the real input consists of the output of the controller and the approximation error. The control object of the designed controller can be considered as a system with input disturbance.

The nonlinear systems with input disturbance can be given as the following state-space representation:

$$\dot{x}(t) = f(x(t)) + g(x(t))\,u(t) + l(x(t))\,w(t), \tag{1}$$

where $x \in \mathbb{R}^n$ denotes the vector of process state variables; $w \in \mathbb{R}^m$ denotes the state disturbance vector; $u \in \mathbb{R}^p$ denotes the control input vector with input disturbance, which can be expanded into $u(t) = u_c(t) + u_e(t)$, $u_c \in \mathbb{R}^p$ denotes the control input vector and $u_e \in \mathbb{R}^p$ denotes the input disturbance. $f : \mathbb{R}^n \to \mathbb{R}^n, g : \mathbb{R}^n \to \mathbb{R}^{n\times p}$, and $l : \mathbb{R}^n \to \mathbb{R}^{n\times m}$ are sufficiently smooth functions. The control input vector u_c is constrained in a convex set $\mathcal{U}_c := \{u_c \in \mathbb{R}^p : |u_c| \leqslant u^{\max}\}$, the input disturbances are bounded as

$$\mathcal{E}_e := \{u_e \in \mathbb{R}^p : |u_e| \leqslant \delta_u\}, \tag{2}$$

where δ_u is a positive constant, and the real control input u is constrained in a convex set $\mathcal{U} := \{u \in \mathbb{R}^p : |u| \leqslant u^{\max} + \delta_u\}$. The state disturbances are bounded as

$$\mathcal{W} := \{w \in \mathbb{R}^m : |w| \leqslant \delta_w\}, \tag{3}$$

where δ_w is a positive constant.

The nominal system can be described by the following state-space model:

$$\dot{x}_n(t) = f(x_n(t)) + g(x_n(t))u_c(t), \tag{4}$$

where the system is considered without disturbances. For simplicity, we use the subscript n to distinguish the real system from the nominal system. For both of these systems, we assume that f, g, l and k are locally Lipschitz vector functions and $f(0) = 0, k(0) = 0$.

2.3 Lyapunov-based controller

For the systems mentioned above, we assume that there exists a Lyapunov-based controller $h(x_n) = u_c$ that renders the origin of the nominal system of (4) is asymptotically stable for all the states x_n inside a given region Ω_ρ. And Ω_ρ is the stability region for the closed-loop system under the control of $h(x_n)$. According to the converse Lyapunov theorems, we can find a continuously differentiable function $V(x_n)$ and class $\mathcal{K}$ functions $\alpha_i(\cdot), i = 1, 2, 3, 4$ that satisfy the following inequalities:

$$\alpha_1(|x_n|) \leqslant V(x_n) \leqslant \alpha_2(|x_n|), \tag{5a}$$

$$\frac{\partial V(x_n)}{\partial x_n}(f(x_n) + g(x_n)h(x_n)) < -\alpha_3(|x_n|), \tag{5b}$$

$$\left|\frac{\partial V(x_n)}{\partial x_n}\right| \leqslant \alpha_4(|x_n|), \tag{5c}$$

$$h(x_n) \in \mathcal{U}_c. \tag{5d}$$

Remark 1. In this paper, we choose the Sontag control law as $h(x_n) = [h_1(x_n), h_2(x_n), \ldots, h_p(x_n)]^{\mathrm{T}}$, which can be given as

$$h_i(x_n) = \begin{cases} -\dfrac{L_f V + \sqrt{L_f V^2 + \gamma |L_g V|^4}}{|L_g V|^2} L_{g_i} V, & |L_g V(x_n)| \neq 0, \\ 0, & |L_g V(x_n)| = 0, \end{cases} \tag{6}$$

where $\gamma > 0$ and $g = [g_1, g_2, \ldots, g_p], g_i(\cdot) : \mathbb{R}^n \to \mathbb{R}^n$. The stability of the closed-loop system under the control law $h(x_n)$ is ensured and the detailed proof is similar to that in [26].

The Lyapunov function $V(x_n)$ can be expressed as $V(x_n) = x_n^{\mathrm{T}} P x_n$, where $P \in \mathbb{R}^{n\times n}$ is a positive definite constant matrix. According to (5), we can obtain a region where $\dot{V}$ is rendered negetive under the controller $h(x_n)$ and we define $\mathbb{H}_c = \{x_n \in \mathbb{R}^n | \dot{V}(x_n) = L_f V + L_g V u_c < -kV(x_n), u_c = h(x_n) \in \mathbb{U}_c\} \cap \{0\}$, where k is a positive real number. Then, we give the definition of the closed-loop stability region Ω_ρ as $\Omega_\rho := \{x_n \in \mathbb{H}_c | V(x_n) \leqslant \rho\}$, where $\rho > 0$ and $\Omega_\rho \subset \mathbb{H}_c$. To obtain Ω_ρ, with considering that the system is a Lipschitz vector function, we can go through each possible state with small distance to check if the state belong to $\mathbb{H}_c$. An irregular region represents $\mathbb{H}_c$ in state space can be obtained. Then, provided certain V, the largest ρ such that $\Omega_\rho \subset \mathbb{H}_c$ can be obtained by linear searching method.

For $x \in \Omega_\rho$, according to the Lipschitz property of f, g, l and boundedness of u, w, there exists a positive constant M that satisfies

$$|f(x(t)) + g(x(t))u(t) + l(x(t))w(t)| \leqslant M. \tag{7}$$

Consider the continuously differentiable property of $V(x_n)$ and the Lipschitz property assumed for f, g, l. The following inequalities are available:

$$|(f(x) + g(x)u + l(x)w) - (f(x_n) + g(x_n)u_c)| \leqslant L_f|x - x_n| + L_g|x - x_n|u^{\max} + L_l\delta_w + M_g\delta_u, \tag{8a}$$

$$\begin{aligned} &\left|\frac{\partial V(x)}{\partial x}(f(x) + g(x)u + l(x)w) - \frac{\partial V(x_n)}{\partial x}(f(x_n) + g(x_n)u_c)\right| \\ &\leqslant L_{fv}|x - x_n| + L_{gv}|x - x_n|u^{\max} + L_{lv}\delta_w + M_{gv}\delta_u, \end{aligned} \tag{8b}$$

where L_f, L_g, L_l are Lipschitz constants associated with functions f, g, l; L_{fv}, L_{gv}, L_{lv} are the Lipschitz constants associated with functions $L_f V, L_g V, L_l V$; M_g is the maximum value of the function g; M_{gv} is the maximum value of the function $L_g V$.

The control objective is to ensure the stability of the closed-loop system under the influence of the input disturbance. Then the controller can be realized by some approximate methods with bounded errors for high sampling rate.

3 LMPC with input disturbance

3.1 Formulation

In this subsection, a set of indispensable stability constraints are included in the design of the MPC controller to guarantee the stability of the closed-loop system. And the MPC controller is designed via LMPC techniques, where the practical stability of the closed-loop system and the reduction of the complexity in the optimization problem are guaranteed.

Considering the input disturbance, the controller $h(x)$ is used to define a stability constraint for the LMPC controller. Therefore, the parameters of LMPC should be designed to satisfy a certain condition where the affection of the input disturbance is considered so that the controller can inherit the stability and robustness properties of the Lyapunov-based controller $h(x)$ and the convergence region of the state can satisfy the state constraints. Furthermore, the input constraint should be a reduced set of $\mathcal{U}_c$.

The optimization problem of the proposed LMPC is formulated as follows:

$$\min_{u_c \in S(\Delta)} \int_{t_k}^{t_{k+N}} L(\tilde{x}_n(\tau), u_c(\tau))\mathrm{d}\tau \tag{9a}$$

s.t.

$$\dot{\tilde{x}}_n(\tau) = f(\tilde{x}_n(\tau)) + g(\tilde{x}_n(\tau))u_c(\tau), \tag{9b}$$

$$u_c(\tau) \in \mathcal{U}_c, \tag{9c}$$

$$\tilde{x}_n(t_k) = x(t_k), \tag{9d}$$

$$\frac{\partial V(x(t_k))}{\partial x} g(x(t_k))u_c(t_k) \leqslant \frac{\partial V(x(t_k))}{\partial x} g(x(t_k))h(x(t_k)), \tag{9e}$$

where Δ is the sampling period and the $t_k = k\Delta$ is the sampling instant; the optimal variable $u_c \in S(\Delta)$ takes piece-wise constant values that expressed as $u_c(\tau) = u_c^*(\tau|t_k), \tau \in [t_k, t_{k+N})$, and $S(\Delta)$ is the family of piece-wise continuous functions with the period Δ; $L(\cdot,\cdot)$ is the optimization object that needs to be minimized; N is the control prediction horizon; $\tilde{x}_n$ is the predicted trajectory of the system. Constraint (9b) is used to predict the state trajectory of the nominal system; constraint (9c) limits the optimal control input u_c; constraint (9d) defines the initial condition of the optimal problem.

If the predicted state $\tilde{x}_n$ is always kept in Ω_{ρ_e}, then the actual state x will always be maintained in Ω_ρ. The relationship between Ω_{ρ_e} and Ω_ρ will be characterized in Theorem 1. Considering the effects of the bounded disturbances w and u_e, one important problem is how to define the region Ω_{ρ_e} that ensures the stability of the system with the control of LMPC and satisfies the following inequality:

$$\rho_e \geqslant \max\left\{V(x(t+\Delta)) : V(x(t)) \leqslant \rho_s\right\}, \tag{10}$$

where ρ_s is a small region that satisfies the robustness under the control of $h(x)$ during the sampling time Δ for $x \in \Omega_\rho/\Omega_{\rho_e}$, and the following inequation should hold as the disturbances are considered:

$$-\alpha_3(\alpha_2^{-1}(\rho_s)) + (L_{fv} + L_{gv}u^{\max})M\Delta + M_{lv}\delta_w + M_{gv}\delta_u \leqslant -\varepsilon_w/\Delta. \tag{11}$$

In this paper, we consider two cases: the first one is LMPC, where the states are driven to the setpoints; the second one is Lyapunov-based Economic MPC (LEMPC) for obtaining economic performance, where the economic cost function is considered. And the constraint (9e) should be modified as

$$V(\tilde{x}_n(\tau)) \leqslant \rho_e,\ \forall \tau \in [t_k, t_{k+N}),\ \text{if } t_k \leqslant t' \text{ and } V(x(t_k)) \leqslant \rho_e, \tag{12a}$$

$$\frac{\partial V(x(t_k))}{\partial x} g(x(t_k))u_c(t_k) \leqslant \frac{\partial V(x(t_k))}{\partial x} g(x(t_k))h(x(t_k)),\ \text{if } t_k > t' \text{ or } \rho_e < V(x(t_k)) \leqslant \rho. \tag{12b}$$

Case 1. For the implementation of LMPC for tracking, constraint (9e) is effective so that the Lyapunov function of the system decreases faster than that of the system with piece-wise constant control $h(x(t_k))$. Under this circumstance, the convergence of the closed-loop system is guaranteed so that the state of the closed-loop system can be forced into Ω_{ρ_s} within finite steps. Here, ρ_e is a small value, slightly larger than ρ_s.

Case 2. For the implementation of LEMPC, the optimal process can be divided into two modes. A specific time t' is set here to distinguish the time period of the two modes. From the initial time t_0 up to t', the LEMPC operates in the first mode, where the constraint (12a) is effective so that the economic cost is optimized if the sampled state $x(t_k)$ is kept in Ω_{ρ_e}; if the sampled state $x(t_k)$ is out of Ω_{ρ_e} but kept in Ω_ρ or the time instant is after t', the LEMPC operates in the second mode, where the constraint (12b) is effective so that the state of the closed-loop system can be enforced into the stability region in a finite time. In this circumstance, ρ_e can be much larger than ρ_s for the state of the system is only required to be regulate within a zone.

3.2 Stability

In this subsection, two propositions and one theorem will be given to analyze the stability of the system with the effects of the input disturbance u_e we mentioned above.

Proposition 1. Considering the system of (1) and (4), assume the initial states $x(t_0) = x_n(t_0) \in \Omega_\rho$. There exists a $\mathcal{K}$ function $f_w(\cdot,\cdot)$ satisfying

$$|x_n(t) - x(t)| \leqslant f_w(\delta_u, t - t_0) \tag{13}$$

for all $x(t), x_n(t) \in \Omega_\rho$ and $u_e(t) \in \mathcal{E}_e$, $w(t) \in \mathbb{W}$ with

$$f_w(\delta_u, t - t_0) = \frac{M_l\delta_w + M_g\delta_u}{L_f + L_g u^{max}}\left[\mathrm{e}^{(L_f + L_g u^{\max})(t - t_0)} - 1\right]. \tag{14}$$

The proposition above gives an upper bound of the deviation between the actual system and nominal system under the same control input, and this upper bound takes into account the effects of the input disturbance u_e and process disturbance w.

Proof. Let $e_x = x_n - x$, and thus the time derivative of e_x can be described as

$$\begin{aligned}\dot{e}_x &= \dot{x}_n - \dot{x} \\ &= f(x_n) + g(x_n)u_c(t) - f(x) - g(x)u(t) - l(x)w(t).\end{aligned} \tag{15}$$

Based on the Lipschitz property of f, g and the boundedness of u_e, w and u_c, $\dot{e}_x$ is bounded as

$$\begin{aligned}|\dot{e}_x| &\leqslant L_f\,|e_x| + L_g u_c(t)\,|e_x| + |g(x)u_e(t)| + |l(x)w(t)| \\ &\leqslant (L_f + L_g u^{\max})\,|e_x| + M_g\delta_u + M_l\delta_w,\end{aligned} \tag{16}$$

where M_g, M_l are positive constants associated with functions g, l.

Considering that $e_x(t_0) = x_n(t_0) - x(t_0) = 0$, it is proved that

$$|e_x(t)| \leqslant \frac{M_l\delta_w + M_g\delta_u}{L_f + L_g u^{\max}}\left[\mathrm{e}^{(L_f + L_g u^{\max})(t-t_0)} - 1\right]. \tag{17}$$

Proposition 2. Considering the system of (1), there exists a quadratic function $f_v(\cdot)$ that satisfies

$$V(x_1) - V(x_2) \leqslant f_v(|x_1 - x_2|) \tag{18}$$

for all $x_1, x_2 \in \Omega_\rho$ with

$$f_v(s) = \alpha_4(\alpha_1^{-1}(\rho))s + M_v s^2, \tag{19}$$

where M_v is a positive constant.

This proposition limits the difference of the Lyapunov function between two different states in Ω_ρ [27].

Theorem 1. Considering the system of (1) under the control of the proposed LMPC (9) for LEMPC, the Lyapunov-based constraints (12) should be considered. Let $\varepsilon_w > 0, \Delta > 0$ and $0 < \rho_s < \rho_{\min} < \rho_e < \rho$, which satisfies

$$\rho_e \leqslant \rho - f_v(f_w(\delta_u, \Delta)), \tag{20}$$

$$-\alpha_3(\alpha_2^{-1}(\rho_s)) + (L_{fv} + L_{gv}u^{\max})M\Delta + M_{lv}\delta_w + M_{gv}\delta_u \leqslant -\varepsilon_w/\Delta, \tag{21}$$

and

$$\rho_{\min} = \max\left\{V(x(t+\Delta)) : V(x(t)) \leqslant \rho_s\right\}. \tag{22}$$

If $x(t_0) \in \Omega_\rho$, the state variable $x(t)$ will always be bounded in Ω_ρ and be ultimately bounded in $\Omega_{\rho_{\min}}$.

Proof. We prove the stability for the above two cases. First of all, we will give the feasibility analysis. For LEMPC, the proof consists of three parts. The first one proves that if $t_k \in [t_0, t')$ and $x(t_k) \in \Omega_{\rho_e}$, the state $x(t_{k+1})$ will always be bounded in Ω_ρ. The second one proves that if $t_k \in [t_0, t')$ and $x(t_k) \in \Omega_\rho/\Omega_{\rho_e}$, the state $x(t), t \in [t_k, t_{k+1})$ will be ultimately bounded in Ω_{ρ_e}. The third one proves that if $t_k \geqslant t'$ and $x(t_k) \in \Omega_\rho$, the state $x(t)$ will be ultimately bounded in $\Omega_{\rho_{\min}}$. For LMPC, the proof is similar to Part III.

Feasibility analysis. If $x(t)$ is bounded in Ω_ρ, the feasibility of the LMPC can be ensured since the control law $h(x(t_k))$ can always be a feasible solution that satisfies the input constraint (9c) and the Lyapunov-based constraint (9e). Similarly, the control law $h(x(t_k))$ still satisfies the Lyapunov-based contraints (12a) and (12b). The premise of this condition (i.e., the state $x(t)$ is always maintained in Ω_ρ) will be proved in the following parts.

Part I. During the first operation mode, if $x(t_k) \in \Omega_{\rho_e}$, then $x(t_{k+1}) \in \Omega_\rho$. According to the Propositions 1 and 2, the relationship of the Lyapunov functions between the actual state $x(t_{k+1})$ and the predictive state $\tilde{x}_n\,(t_{k+1})$ can be obtained:

$$V(x(t_{k+1})) \leqslant V(\tilde{x}(t_{k+1})) + f_v(f_w(\delta_u, \Delta)). \tag{23}$$

Considering the condition of (20) and $V(\tilde{x}(t_{k+1})) \leqslant \rho_e$ are satisfied, thus $x(t_{k+1}) \in \Omega_\rho$ can be ensured.

Part II. During the first operation mode, if $x(t_k) \in \Omega_\rho/\Omega_{\rho_e}$, then $x(t)$ will be bounded in Ω_{ρ_e} based on the control of LMPC.

Considering the constraint of (9e) and the inequalities of (5),

$$\begin{aligned}&\frac{\partial V\left(x_n\left(t_k\right)\right)}{\partial x}\left(f\left(x_n\left(t_k\right)\right)+g\left(x_n\left(t_k\right)\right)u_c\left(t_k\right)\right)\\&\leqslant\frac{\partial V\left(x_n\left(t_k\right)\right)}{\partial x}\left(f\left(x_n\left(t_k\right)\right)+g\left(x_n\left(t_k\right)\right)h\left(x_n\left(t_k\right)\right)\right)\\&\leqslant-\alpha_3\left(\left|x_n\left(t_k\right)\right|\right).\end{aligned}\tag{24}$$

For the actual system of (1), the time derivative of the Lyapunov function can be obtained as

$$\begin{aligned}\dot V(x(t))&=\frac{\partial V(x(t))}{\partial x}(f(x(t))+g(x(t))u(t)+l(x(t))w(t))\\&\leqslant\frac{\partial V(x(t))}{\partial x}(f(x(t))+g(x(t))u(t_k)+l(x(t))w(t))\\&\quad-\frac{\partial V\left(x_n\left(t_k\right)\right)}{\partial x}(f(x_n(t_k))+g(x_n(t_k))u_c(t_k))-\alpha_3(|x_n(t_k)|).\end{aligned}\tag{25}$$

Taking into account that $x(t_k)=x_n(t_k)$ and the boundedness of $\dot x$ expressed in (7),

$$\dot V\left(x\left(t\right)\right)\leqslant-\alpha_3\left(\left|x\left(t_k\right)\right|\right)+\left(L_{fv}+L_{gv}\right)M\Delta+M_{gv}\delta_u+M_{lv}\delta_w.\tag{26}$$

Let $\rho_s<\rho_e$, and thus $x(t_k)\in\Omega_\rho/\Omega_{\rho_s}$ is satisfied. According to the the properties of the Lyapunov function listed in (5),

$$\dot V\left(x\left(t\right)\right)\leqslant-\alpha_3\left({\alpha_2}^{-1}\left(\rho_s\right)\right)+\left(L_{fv}+L_{gv}\right)M\Delta+M_{gv}\delta_u+M_{lv}\delta_w.\tag{27}$$

If Eq. (11) is satisfied, for $t\in[t_k,t_{k+1})$,

$$\dot V\left(x\left(t\right)\right)\leqslant-\varepsilon_w/\Delta,\tag{28}$$

we can obtain that

$$\begin{aligned}V\left(x\left(t\right)\right)&\leqslant V\left(x\left(t_k\right)\right),\\V\left(x\left(t_{k+1}\right)\right)&\leqslant V\left(x\left(t_k\right)\right)-\varepsilon_w,\end{aligned}\tag{29}$$

which proves that the state $x(t)$ will be bounded in the stability region Ω_ρ forever and converge to Ω_{ρ_e} in a finite number of sampling times.

Part III. During the second operation mode, if $x(t_k)\in\Omega_\rho$, then the Lyapunov function satisfies $V(x(t_{k+1}))\leqslant V(x(t_k))$ and the state will be bounded in $\Omega_{\rho_{\min}}$ ultimately.

If $x(t_k)\in\Omega_\rho/\Omega_{\rho_s}$, the proofs shown in Part II is equally applicable and Eq. (29) is valid. Therefore, we can obtain that the state variable $x(t)$ will converge to Ω_{ρ_s} with a finite number of sampling times. For the definition of $\rho_{\min}$, if $x(t)\in\Omega_{\rho_s}$, the state at the next sampling point $x(t+\Delta)$ will be bounded in $\Omega_{\rho_{\min}}$. Therefore, the state $x(t)$ will be ultimately bounded in $\Omega_{\rho_{\min}}$ for $x(t_k)\in\Omega_\rho$ in the second operation mode.

The relationship of these regions is given in Figure 2. We can see Ω_{ρ_e} shrinks and Ω_{ρ_s} extends. Ω_ρ represents the stability region defined for the whole process, which means that the actual state of the system $x(t_k)$ can be chosen in Ω_ρ to ensure the stability for the period $[t_k,t_{k+1})$.

Remark 2. Since the control law $h(x)$ we used in this paper satisfies the input constraint (5d), the region Ω_ρ can be constracted without the influence of input disturbance. Considering the construction of Ω_ρ, it will remain the same if $V(x)$ and $h(x)$ remain unchanged.

4 Implementation

If a high sampling rate is required in the control structure, the online optimization may get computationally intractable due to the burden under the online requirement. We approximate each local nonlinear MPC controller κ_{MPC} by a mapping function expressed as κ_{map}, which guarantees the execution efficiency of the controllers by learning methods. The state variables x serve as the inputs in κ_{map}. u is the output of κ_{map} that is expected to be equal to the output of κ_{MPC} (i.e., the control input u_c). Then we use

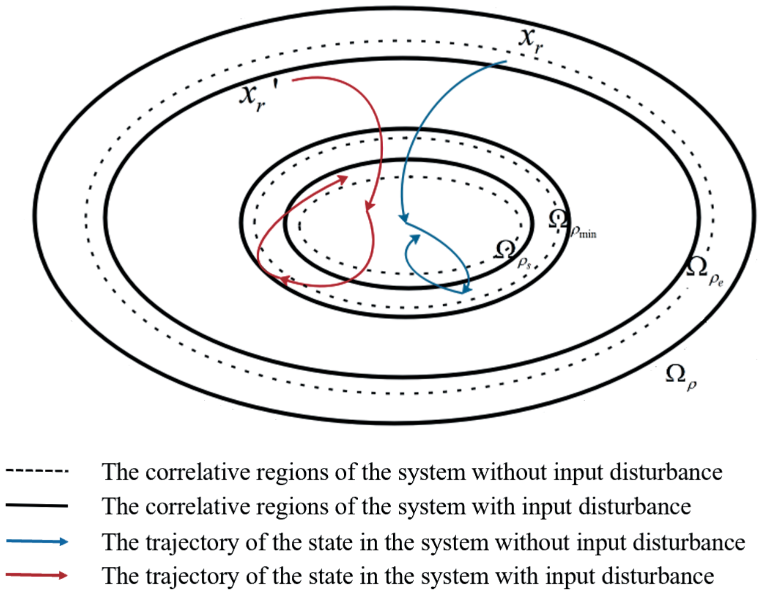

Figure 2 (Color online) The relationship of the regions.

Hoeffding's inequality to ensure that the fitting errors are small enough to guarantee the feasibility of the approximated controllers at a certain confidence level. The procedure is shown as follows:

(1) Given the lower bound of probabilistic μ_l to ensure the closed-loop system feasible, sample the data of the MPC controller κ_{MPC} offline;

(2) Learning: $\kappa_{\text{map}}(x) \approx \kappa_{\text{MPC}}(x)$;

(3) Validate $\kappa_{\text{map}}(x)$ based on Hoeffding's inequality;

(4) If validated, the $\kappa_{\text{map}}(x)$ is feasible; else, change the parameters (i.e., increase the sample size r), and goto (4).

During the process of validating the approximation of the κ_{map}, we need to determine whether $x(t_k)$ and κ_{map} satisfy the constraints. Consider the $X_p := \{x(t), u(t) : u = \kappa_{\text{map}}(x)\}$. The following indicator function is defined to indicate whether the state in X_p is an effective one:

$$I(X_p) := \begin{cases} 1, & u(t) \in \mathcal{U}, \\ 0, & u(t) \notin \mathcal{U}. \end{cases} \tag{30}$$

Consider r as the sample size, $X_p, p = 1, 2, \ldots, r$, and assume that the initial condition of any sampling is independent and identically distributed. Then the empirical risk is

$$\tilde{\mu} := \frac{1}{r} \sum_{p=1}^{r} I(X_p). \tag{31}$$

For any X_p, the feasibility and stability are guaranteed if $I(X_p) = 1$. Let $\mu := P[I(X_p) = 1]$. Hoeffding's inequality is used to estimate μ from $\tilde{\mu}$ as follows:

$$P[|\tilde{\mu} - \mu| \geqslant \varepsilon_h] \leqslant 2\exp\left(-2r{\varepsilon_h}^2\right). \tag{32}$$

Let $\delta_h = 2\exp(-2r\varepsilon_h^2)$ serve as the confidence level and δ_h be given for the desired target. So $P[I(X_p) = 1] = \mu \geqslant \tilde{\mu} - \varepsilon_h$ is tenable with the confidence of at least $1 - \delta_h$. We give the lower bound of probabilistic μ_l to guarantee the validity of the fitting results:

$$P[I(X_p) = 1] = \mu \geqslant \tilde{\mu} - \varepsilon_h \geqslant \mu_l, \tag{33}$$

where μ_l is also given for the desired target. The number of the state r can be adjusted to meet the requirement. If Eq. (33) is satisfied, the validation is successful. If Eq. (33) is failed, we increase r until Eq. (33) is satisfied. We set the maximum number of r to avoid getting stuck, and the fitting invalid if r exceeds the maximum number.

Table 1 Parameters value

Symbol	Meaning	Value
F	Inlet flow rate	$5\ \mathrm{m}^3\cdot\mathrm{h}^{-1}$
T_0	Inlet temperature	300 K
V	Reactor volume	$1\ \mathrm{m}^3$
ΔH	Heat of reaction	$1.15\times10^4\ \mathrm{kJ}\cdot\mathrm{kmol}^{-1}$
k_0	Pre-exponential factor	$8.46\times10^6\ \mathrm{h}^{-1}$
E	Activation energy	$5\times10^3\ \mathrm{kJ}\cdot\mathrm{kmol}^{-1}$
R	Gas constant	$8.314\ \mathrm{kJ}\cdot\mathrm{kmol}^{-1}\cdot\mathrm{K}^{-1}$
σ	Liquid density	$1000\ \mathrm{kg}\cdot\mathrm{m}^{-3}$
C_p	Heat capacity	$0.231\ \mathrm{kJ}\cdot\mathrm{kg}^{-1}\cdot\mathrm{K}^{-1}$
Q_s	Heat rate supplied to the reactor	$1.73\times10^5\ \mathrm{kJ}\cdot\mathrm{h}^{-1}$
C_{As}	Steady-state concentration	$2.44\ \mathrm{kmol}\cdot\mathrm{m}^{-3}$
C_{A0s}	Steady-state inlet concentration	$5\ \mathrm{kmol}\cdot\mathrm{m}^{-3}$
T_s	Steady-state temperature	321.95 K

Remark 3. To ensure the reliability of the approximated control law κ_{map}, we randomly select enough points in the stable region Ω_ρ for the approximation. And the distance between each selected point is required to be as small as possible to achieve the full coverage of the region. Therefore, κ_{map} is designed for dealing with initial states x_0 within Ω_ρ. However, $l\kappa_{\mathrm{map}}$ should be retrained under some circumstances (e.g., the economic cost function changes in the LEMPC or the Lyapunov-based control law $h(x)$ changes).

5 Simulation

In this section, we consider a well-mixed, non-isothermal continuous stirred tank reactor (CSTR) with

$$\frac{\mathrm{d}C_A}{\mathrm{d}t}=\frac{F}{V}\left(C_{A0}-C_A\right)-k_0\mathrm{e}^{-\frac{E}{RT}}{C_A}^2, \tag{34a}$$

$$\frac{\mathrm{d}T}{\mathrm{d}t}=\frac{F}{V}\left(T_0-T\right)-\frac{\Delta H}{\sigma C_p}k_0\mathrm{e}^{-\frac{E}{RT}}{C_A}^2+\frac{Q}{\sigma C_p V}, \tag{34b}$$

where C_A is the concentration and T is the temperature in the reactor. Let C_{As} and T_s denote the concentration and temperature under steady-state, respectively, and then the states are defined as $x=[C_A-C_{As}\quad T-T_s]^{\mathrm{T}}$; C_{A0} is the inlet reactant concentration and C_{A0s} is defined as the variable associated with the steady-state; Q is the external heat input/removal and Q_s is defined as the heat under steady-state. The inputs are defined as $u=[u_1\quad u_2]^{\mathrm{T}}=[C_{A0}-C_{A0s}\quad Q-Q_s]^{\mathrm{T}}$. The process parameters are listed in Table 1.

The available inputs are defined in the following convex set: $\mathbb{U}:=\{u\in\mathbb{R}^2:|u_1|\leqslant3.5\ \mathrm{kmol}\cdot\ \mathrm{m}^3,|u_2|\leqslant 4.85\times10^5\ \mathrm{kJ}\cdot\ \mathrm{h}\}$ and the Lyapunov-based control law is chosen as the Sontag control law we mentioned in Remark 1.

We consider two cases: the first one is LMPC for tracking, the second one is LEMPC, where the economic cost function is maximized. The specific parameters of the simulation, the desired set points and the economic objective will be given in Subsections 5.2 and 5.3.

5.1 Controller approximation

A back propagation neural network (BPNN) with seven neurons in the first hidden layer and five neurons in the second layer is adopted as the learning method to get the approximation of the LMPC. The two states C_A-C_{As} and $T-T_s$ are the inputs of the BPNN. The approximation error that is considered as the input disturbance should be chosen reasonably so that the stability regions can be founded. In this study, we choose $\delta_u=[1.5\times10^{-2},2\times10^2]^{\mathrm{T}}$. For approximation, 2×10^6 data points (x_n,u_n) are sampled under the stable circumstance to create the learning samples, which are initialized randomly in the stability region Ω_ρ for the reliability of the data.

Case 1. The approximation results of $\kappa_{\mathrm{map}}(x)$ in LMPC are shown in Figure 3.

Case 2. The approximation results of $\kappa_{\mathrm{map}}(x)$ in LEMPC are shown in Figure 4.

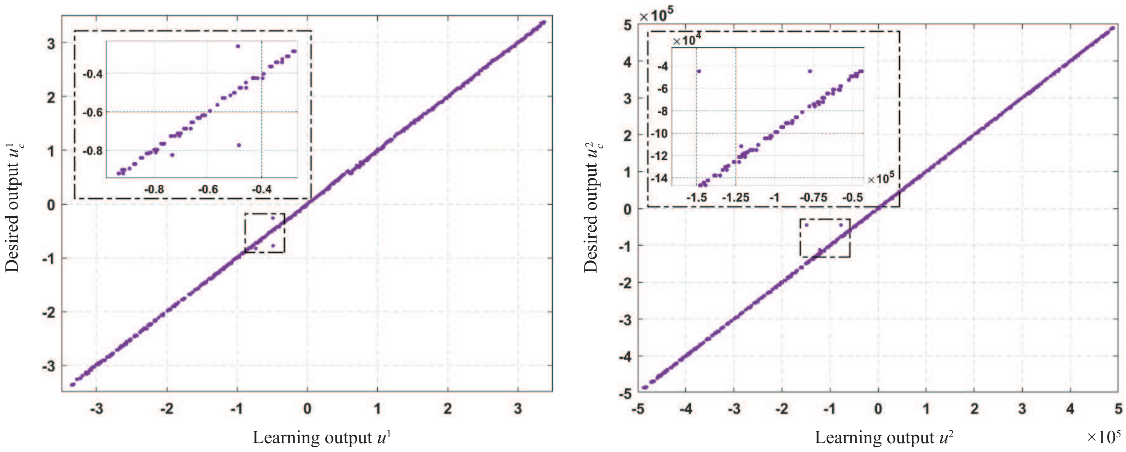

Figure 3 (Color online) Approximation of the proposed LMPC controller.

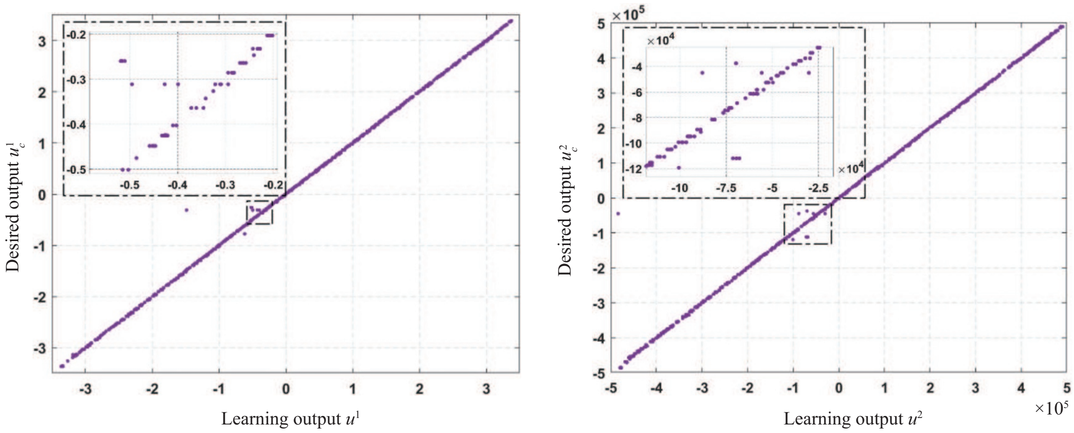

Figure 4 (Color online) Approximation of the proposed LEMPC controller.

To validate if the approximator satisfies Hoeffding's inequality, we set the confidence of $P\left[I(X_p)=1\right]$ as 99% and choose $\delta_h=0.01$ and the lower bound $\mu_l=0.99$.

Case 1. For the $\kappa_{\rm MPC}$ in LMPC for tracking, to satisfy (33), we increase the sample size r to 52030, and the empirical risk is $\tilde{\mu}=[0.99753, 0.99736]$.

Case 2. For the $\kappa_{\rm MPC}$ in LEMPC, to satisfy (33), we increase the sample size r to 53500, and the empirical risk is $\tilde{\mu}=[0.99013, 0.99011]$.

To prove the efficiency of the approximation method, we choose 1000 random initial points over the stable region in the two cases, and then we compare the online processing time between the control law $\kappa_{\rm MPC}$ and $\kappa_{\rm map}$ under the same circumstance.

Case 1. The LMPC took 0.8325 s on average and the approximate controller $\kappa_{\rm map}$ took 0.0042 s. The computational efficiency is increased by about 230 times.

Case 2. The LEMPC took 1.2532 s on average and the approximate controller $\kappa_{\rm map}$ took 0.0061 s. The computational efficiency is increased by about 200 times.

5.2 Performance of the LMPC considering input disturbance

In the simulation, the optimal objective is to minimize the tracking error, and the stage cost function is

$$L\left(x,u_i\right)=\|C_A-C_{As}\|_{10}^2+\|T-T_s\|_1^2. \tag{35}$$

We set the starting time $t_0=0$ h and the final time $t_f=0.3$ h. The sampling period $\Delta=0.01$ h. The LMPC horizon is chosen to be $N=10$. A quadratic Lyapunov function $V(x)=x^{\rm T}Px$ with $P=[[1060\quad 22]^{\rm T}\quad [22\quad 0.52]^{\rm T}]$ is considered.

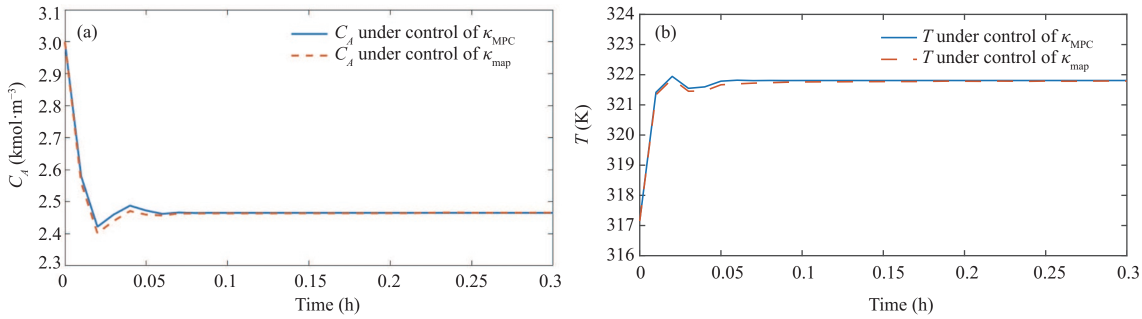

Figure 5 (Color online) The trajectories of C_A (a) and T (b) under control of the proposed LMPC ($\kappa_{\rm MPC}$) and corresponding approximator ($\kappa_{\rm map}$).

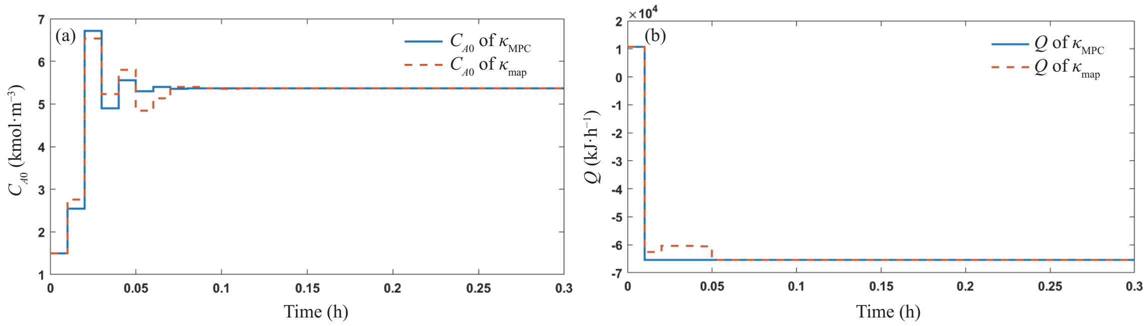

Figure 6 (Color online) The variations of C_{A0} (a) and Q (b) under control of the proposed LMPC ($\kappa_{\rm MPC}$) and corresponding approximator ($\kappa_{\rm map}$).

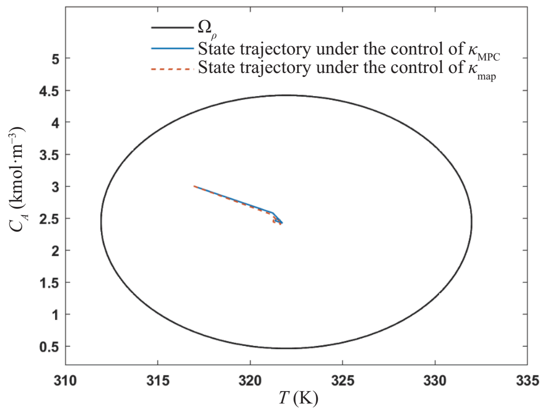

Figure 7 (Color online) The state trajectories under control of the proposed LMPC ($\kappa_{\rm MPC}$) and corresponding approximator ($\kappa_{\rm map}$).

We set the initial states as $x_0 = [0.56, -4.7]^{\rm T}$, and the control objective is steering the states to the origin (i.e., the equilibrium point $C_{As} = 2.44$ kmol $\cdot$ m^{-3}, $T_s = 321.95$ K).

The resulting C_A and T are shown in Figure 5. The trajectories of them are given under the control of the $\kappa_{\rm MPC}$ and $\kappa_{\rm map}$, respectively. It can be seen that under the influence of the approximation error (i.e., input disturbance), the states can be stabilized and the differences between the steady states are acceptable. The $L(x, u)$ of $\kappa_{\rm MPC}$ is 0.988 while the $L(x, u)$ of $\kappa_{\rm map}$ is 1.030 which is 3.51% more than that of $\kappa_{\rm MPC}$. The variations of the inlet reactant concentration C_{A0} and the exchange of the external heat Q are shown in Figure 6.

The stability region Ω_ρ can be derived according to the definition given in Remark 1. The result is depicted as Figure 7. The state trajectories x and x' are always bounded in Ω_ρ and tend to the steady-state with the actions of the $\kappa_{\rm MPC}$ and $\kappa_{\rm map}$.

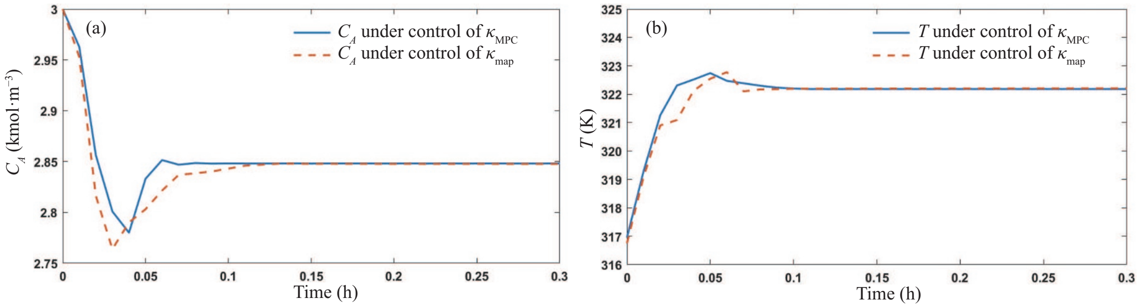

Figure 8 (Color online) The trajectories of C_A (a) and T (b) under control of the proposed LEMPC ($\kappa_{\rm MPC}$) and corresponding approximator ($\kappa_{\rm map}$).

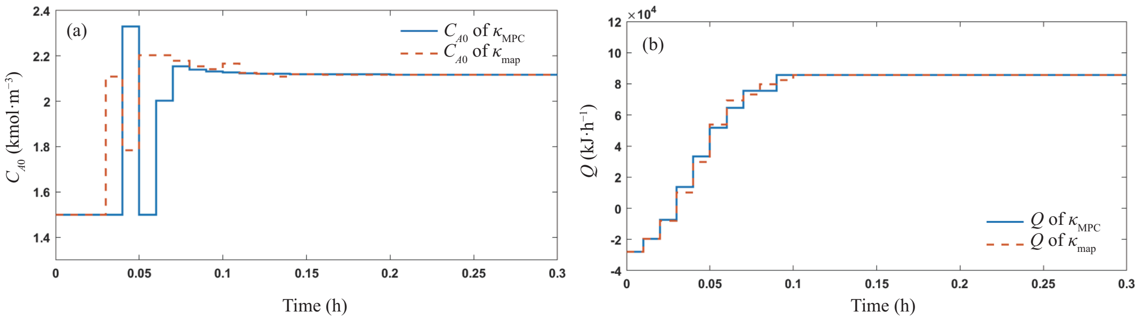

Figure 9 (Color online) The variations of C_{A0} (a) and Q (b) under control of the proposed LEMPC ($\kappa_{\rm MPC}$) and corresponding approximator ($\kappa_{\rm map}$).

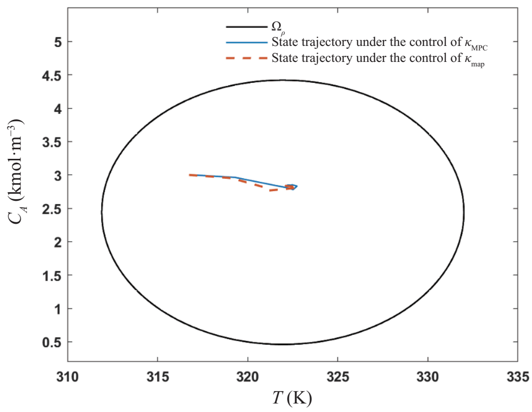

Figure 10 (Color online) The state trajectories under control of the proposed LEMPC ($\kappa_{\rm MPC}$) and corresponding approximator ($\kappa_{\rm map}$).

5.3 Performance of the LEMPC considering input disturbance

In this case, the economic objective is to maximize the reactant rate by manipulating the inputs over the whole process for t_f, and the economic cost function of LEMPC can be formulated as

$$L\left(x, u_i\right) = -k_0 \mathrm{e}^{-\frac{E}{RT}} C_A^2. \tag{36}$$

We set the same simulation parameters as that in LMPC. And we also set the initial states as $x_0 = [0.56, -4.7]^{\mathrm{T}}$. The resulting C_A and T are shown in Figure 8. Under the control of both the $\kappa_{\rm MPC}$ and $\kappa_{\rm map}$, the states can be stabilized and bounded in the stable regions. The variations of the C_{A0} and Q under the LEMPC controller are shown in Figure 9. The economic cost of the closed-loop system under the control of $\kappa_{\rm MPC}$ is -2.8933×10^5 over the simulation time and the economic cost of $\kappa_{\rm map}$ is -2.8777×10^5. The error is about 0.5% of the system with LEMPC under the control of $\kappa_{\rm map}$.

The stability region Ω_ρ can be depicted as Figure 10. As the initial state is set in Ω_ρ, both of the state trajectories under control of $\kappa_{\rm MPC}$ and $\kappa_{\rm map}$ are bounded in Ω_ρ all the time and tend to the steady-state that maximizes the economic profit with the consideration of the stability.

6 Conclusion

In this paper, the approximate MPC achieved by learning methods can improve the computational efficiency to simplify the process. The statistical error of the approximation is considered as the input disturbance, and the controller is designed via LMPC techniques. The stability of the system is verified if the input disturbance is limited within a certain range, and the influence of the inaccurate inputs is reflected in the variation of the stability regions.

Acknowledgements This work was supported by National Key R&D Program of China (Grant No. 2018AAA0101701) and National Natural Science Foundation of China (Grant Nos. 62073220, 61833012).

References

1 Qi W, Liu J F, Chen X Z, et al. Supervisory predictive control of standalone wind/solar energy generation systems. IEEE Trans Contr Syst Technol, 2011, 19: 199–207

2 Rigatos G, Abbaszadeh M, Siano P, et al. Nonlinear optimal control of electro-hydraulic actuators. IFAC J Syst Control, 2021, 15: 100130

3 Song R Z, Xiao W D, Sun C Y. A new self-learning optimal control laws for a class of discrete-time nonlinear systems based on ESN architecture. Sci China Inf Sci, 2014, 57: 068202

4 Zhang Z, Li H P, Shi Y, et al. Cooperative optimal control for Lipschitz nonlinear systems over generally directed topologies. Automatica, 2020, 122: 109279

5 Liu X J, Kong X B. Nonlinear model predictive control for DFIG-based wind power generation. IEEE Trans Automat Sci Eng, 2014, 11: 1046–1055

6 Qin S J, Badgwell T A. A survey of industrial model predictive control technology. Control Eng Practice, 2003, 11: 733–764

7 de la Pena D M, Christofides P D. Lyapunov-based model predictive control of nonlinear systems subject to data losses. IEEE Trans Automat Contr, 2008, 53: 2076–2089

8 Zheng Y, Wei Y S, Li S Y. Coupling degree clustering-based distributed model predictive control network design. IEEE Trans Automat Sci Eng, 2018, 15: 1749–1758

9 Zheng Y, Li S Y, Tan R M. Distributed model predictive control for on-connected microgrid power management. IEEE Trans Contr Syst Technol, 2018, 26: 1028–1039

10 Hertneck M, Kohler J, Trimpe S, et al. Learning an approximate model predictive controller with guarantees. IEEE Control Syst Lett, 2018, 2: 543–548

11 Drgoňa J, Picard D, Kvasnica M, et al. Approximate model predictive building control via machine learning. Appl Energy, 2018, 218: 199–216

12 Pavlov A, Shames I, Manzie C. Minimax strategy in approximate model predictive control. Automatica, 2020, 111: 108649

13 Zhang H, Li S Y, Zheng Y. Q-learning-based model predictive control for nonlinear continuous-time systems. Ind Eng Chem Res, 2020, 59: 17987–17999

14 Cseko L H, Kvasnica M, Lantos B. Explicit MPC-based RBF neural network controller design with discrete-time actual Kalman filter for semiactive suspension. IEEE Trans Contr Syst Technol, 2015, 23: 1736–1753

15 Lucia S, Karg B. A deep learning-based approach to robust nonlinear model predictive control. IFAC-PapersOnLine, 2018, 51: 511–516

16 Cao Y K, Gopaluni R B. Deep neural network approximation of nonlinear model predictive control. IFAC-PapersOnLine, 2020, 53: 11319–11324

17 Chen S, Saulnier K, Atanasov N, et al. Approximating explicit model predictive control using constrained neural networks. In: Proceedings of Annual American Control Conference (ACC), 2018. 1520–1527

18 Li D W, Xi Y G. Quality guaranteed aggregation based model predictive control and stability analysis. Sci China Ser F-Inf Sci, 2009, 52: 1145–1156

19 Ruan X G, Hou X Y, Ma H Y. Stability analysis of constrained MPC with CLF applied to discrete-time nonlinear system. Sci China Inf Sci, 2014, 57: 112201

20 Wan R X, Li S Y, Zheng Y. Model predictive control for nonlinear systems with time-varying dynamics and guaranteed Lyapunov stability. Int J Robust Nonlinear Control, 2021, 31: 509–523

21 Xu X, Chen H, Lian C Q, et al. Learning-based predictive control for discrete-time nonlinear systems with stochastic disturbances. IEEE Trans Neural Netw Learn Syst, 2018, 29: 6202–6213

22 Pannocchia G, Rawlings J B, Wright S J. Conditions under which suboptimal nonlinear MPC is inherently robust. Syst Control Lett, 2011, 60: 747–755

23 Allan D A, Bates C N, Risbeck M J, et al. On the inherent robustness of optimal and suboptimal nonlinear MPC. Syst Control Lett, 2017, 106: 68–78

24 Pourdehi S, Karimaghaee P. Stability analysis and design of model predictive reset control for nonlinear time-delay systems with application to a two-stage chemical reactor system. J Process Control, 2018, 71: 103–115

25 Choomkasien P, Chomphooyod P, Banjerdpongchai D. Design of model predictive control for industrial process with input time delay. In: Proceedings of the 17th International Conference on Control, Automation and Systems (ICCAS), 2017. 625–630

26 Sontag E D. A 'universal' construction of Artstein's theorem on nonlinear stabilization. Syst Control Lett, 1989, 13: 117–123

27 Heidarinejad M, Liu J F, Christofides P D. Economic model predictive control using Lyapunov techniques: handling asynchronous, delayed measurements and distributed implementation. In: Proceedings of the 50th IEEE Conference on Decision and Control and European Control Conference, 2011